

## Topological Anderson Insulator

Jian Li,<sup>1,\*</sup> Rui-Lin Chu,<sup>1</sup> J. K. Jain,<sup>2</sup> and Shun-Qing Shen<sup>1</sup>

<sup>1</sup>*Department of Physics and Center of Computational and Theoretical Physics, The University of Hong Kong, Pokfulam Road, Hong Kong*

<sup>2</sup>*Department of Physics, 104 Davey Lab, Pennsylvania State University, University Park, Pennsylvania 16802, USA*  
(Received 18 November 2008; published 1 April 2009)

Disorder plays an important role in two dimensions, and is responsible for striking phenomena such as metal-insulator transition and the integral and fractional quantum Hall effects. In this Letter, we investigate the role of disorder in the context of the recently discovered topological insulator, which possesses a pair of helical edge states with opposing spins moving in opposite directions and exhibits the phenomenon of quantum spin Hall effect. We predict an unexpected and nontrivial quantum phase termed “topological Anderson insulator,” which is obtained by introducing impurities in a two-dimensional metal; here disorder not only causes metal-insulator transition, as anticipated, but is fundamentally responsible for creating extended edge states. We determine the phase diagram of the topological Anderson insulator and outline its experimental consequences.

DOI: 10.1103/PhysRevLett.102.136806

PACS numbers: 73.43.Nq, 72.15.Rn, 72.25.-b, 85.75.-d

Over the last 30 years, investigation of two-dimensional systems has produced a series of striking phenomena and states. A one-parameter scaling theory for noninteracting electrons demonstrates that arbitrarily weak random disorder drives the system into an insulating state, known as the Anderson insulator [1]. In the presence of strong spin orbit coupling or interactions, a metallic state in two dimensions (2D) becomes possible, and a metal-insulator transition occurs at a nonzero critical value of disorder strength [2–4]. The application of a magnetic field, which breaks time-reversal symmetry, creates dissipationless edge states, resulting in the remarkable phenomenon of the integral quantum Hall effect [5]. Interelectron interaction produces the fractional quantum Hall effect [6], characterized by topological concepts such as composite fermions, fractional charge, and fractional statistics [7]. Disorder plays a crucial role in the establishment of the quantized Hall plateaus.

The quantum Hall state constitutes a paradigm for a topological state of matter, the Hall conductance of which is insensitive to continuous changes in the parameters and depends only on the number of edge states, which are unidirectional because of the breaking of the time-reversal symmetry due to the magnetic field. Recently, an analogous effect was predicted in a time-reversal symmetric situation: it was shown that a class of insulators, such as graphene with spin orbit coupling [8] and an “inverted” semiconductor HgTe/CdTe quantum well [9], possess the topological property that they have a single pair of counter-propagating or helical edge states, exhibiting the phenomenon of the quantum spin Hall effect. This “topological insulator” is distinguished from an ordinary band insulator by a  $Z_2$  topological invariant [10], analogous to the Chern number classification of the quantum Hall effect [11]. The edge states are believed to be insensitive to weak (non-magnetic) impurity scattering [10] and weak interaction

[12,13]. The phase diagram for strongly-disordered topological insulators based on graphene has been studied through numerical evaluation of the localization length and the spin Chern number [14,15]. The prediction of nonzero conductance in a band-insulating region of an inverted HgTe/CdTe quantum well has been verified experimentally [16], although the origin of the observed deviation from an exact quantization is not yet fully understood. The topological insulator has also been generalized to three dimensions [17–19].

In view of its importance in 2D, it is natural to ask how disorder affects the stability of the helical edge states in the topological insulator, which has motivated our present study. As expected, we find that the physics of topological insulator is unaffected by the presence of weak disorder but is destroyed for large disorder. More surprisingly, however, our results show that disorder can create a topological insulator for parameters where the system was metallic in the absence of disorder, and also when the band structure of the HgTe/CdTe quantum well is not inverted (i.e., the gap is positive). We call this phase topological Anderson insulator (TAI) and comment on the feasibility of its experimental observation.

The effective Hamiltonian for a clean bulk HgTe/CdTe quantum well is given by [9]

$$\mathcal{H}(\mathbf{k}) = \begin{pmatrix} h(\mathbf{k}) & 0 \\ 0 & h^*(-\mathbf{k}) \end{pmatrix}, \quad (1)$$

where  $h(\mathbf{k}) = \epsilon(k) + \mathbf{d}(\mathbf{k}) \cdot \boldsymbol{\sigma}$ ,  $\mathbf{k} = (k_x, k_y)$  is the two-dimensional wave vector,  $\boldsymbol{\sigma} = (\sigma_x, \sigma_y, \sigma_z)$  are Pauli matrices, and to the lowest order in  $k$ , we have  $\mathbf{d}(\mathbf{k}) = (Ak_x, Ak_y, M - Bk^2)$  and  $\epsilon(k) = C - Dk^2$  with  $A$ ,  $B$ ,  $C$  and  $D$  being sample-specific parameters for which we take realistic values from the experiment [20]. The lower diagonal block  $h^*(-\mathbf{k})$  is the time-reversal counterpart of the upper diagonal block. This four-band model describes

the band mixture of the  $s$ -type  $\Gamma_6$  band and the  $p$ -type  $\Gamma_8$  band near the  $\Gamma$  point. A band inversion results when the gap parameter  $M$  changes its sign from positive to negative. It was predicted that this sign change signifies a topological quantum phase transition between a conventional insulating phase ( $M > 0$ ) and a phase exhibiting the quantum spin Hall effect with a single pair of helical edge states ( $M < 0$ ) [9]; experiments have confirmed some aspects of this prediction [16].

In an infinite-length strip with open lateral boundary conditions, the solution of the four-band model  $\mathcal{H}\Psi = E\Psi$  is given by [21]

$$\Psi(k_x, y) = \left(\frac{1}{\mathcal{T}}\right)(\boldsymbol{\mu}_+ e^{\alpha y} + \boldsymbol{\mu}_- e^{-\alpha y} + \boldsymbol{\nu}_+ e^{\beta y} + \boldsymbol{\nu}_- e^{-\beta y}),$$

where  $\mathcal{T}$  is the time-reversal operator,  $\boldsymbol{\mu}_\pm$  and  $\boldsymbol{\nu}_\pm$  are two-component  $k_x$ -dependent coefficients, and  $\alpha, \beta$  are determined self-consistently by

$$\alpha^2 = k_x^2 + F - \sqrt{F^2 - (M^2 - E^2)/(B^2 - D^2)},$$

$$\beta^2 = k_x^2 + F + \sqrt{F^2 - (M^2 - E^2)/(B^2 - D^2)},$$

$$E_\alpha^2 \beta^2 + E_\beta^2 \alpha^2 - \gamma E_\alpha E_\beta \alpha \beta = k_x^2 (E_\alpha - E_\beta)^2.$$

Here, we have  $F = [A^2 - 2(MB + ED)]/2(B^2 - D^2)$ ,  $E_\alpha = E - M + (B + D)(k_x^2 - \alpha^2)$ ,  $E_\beta = E - M + (B + D)(k_x^2 - \beta^2)$ ,  $\gamma = \tanh\frac{\alpha L_y}{2}/\tanh\frac{\beta L_y}{2} + \tanh\frac{\beta L_y}{2}/\tanh\frac{\alpha L_y}{2}$ , and  $L_y$  is the width of the strip. This solution naturally contains both helical edge states ( $\alpha^2 > 0$ ) and bulk states ( $\alpha^2 < 0$ ), which are shown in Fig. 1 for three cases  $M < 0$ ,  $M = 0$ , and  $M > 0$ . The edge states (red lines in Fig. 1) are seen beyond the bulk gap for all cases, up to an  $M$  dependent maximum energy. When  $M < 0$ , the edge states cross

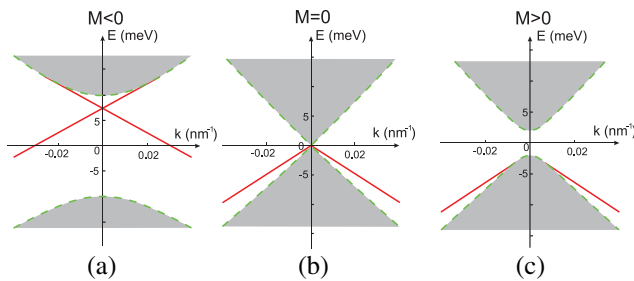


FIG. 1 (color). Band structure of HgTe/CdTe quantum wells with finite width. (a) The “inverted” band structure case with  $M = -10$  meV. Edge states (red lines) cross the bulk band gap and merge into bulk states (gray area) at a maximum energy in the upper band. The green dashed lines mark the boundary of bulk states. (b) The transition point between an inverted band structure and a “normal” band structure with  $M = 0$  meV. (c) The normal band structure with  $M = 2$  meV. In all figures, the strip width  $L_y$  is set to  $100 \mu\text{m}$ . The sample-specific parameters are fixed for all calculations in this Letter to be  $A = 364.5 \text{ meV nm}$ ,  $B = -686 \text{ meV nm}^2$ ,  $C = 0$ ,  $D = -512 \text{ meV nm}^2$ .

the bulk gap producing a topological insulator. At  $M = 0$  the edge states exist only in conjunction with the lower band, terminating at the Dirac point. For positive  $M$  there are no edge states in the gap, producing a conventional insulator [9]. This band picture has been verified also using exact diagonalization of the tight-binding Hamiltonian near the  $\Gamma$  point ( $k = 0$ ).

We next study transport as a function of disorder, with the Fermi energy varying through all regions of the band structure. For this purpose, we use a tight-binding lattice model which produces the above Hamiltonian as its continuum limit [9], and following a common practice in the study of Anderson localization, introduce disorder through random on-site energy with a uniform distribution within  $[-W/2, W/2]$ . We calculate the conductance of disordered strips of width  $L_y$  and length  $L_x$  using the Landauer-Büttiker formalism [22,23]. The conductance  $G$  as a function of disorder strength  $W$  is plotted in Fig. 2 for several values of Fermi energy belonging to different band regions for  $M < 0$  and  $M > 0$ . The topological nature of the system is revealed by the quantization of conductance at  $2e^2/h$ . The following observations can be made.

The calculated behavior conforms to the qualitative expectation for certain situations. For Fermi level in the lower band, for both  $M < 0$  and  $M > 0$ , an ordinary Anderson insulator results when the clean-limit metal is

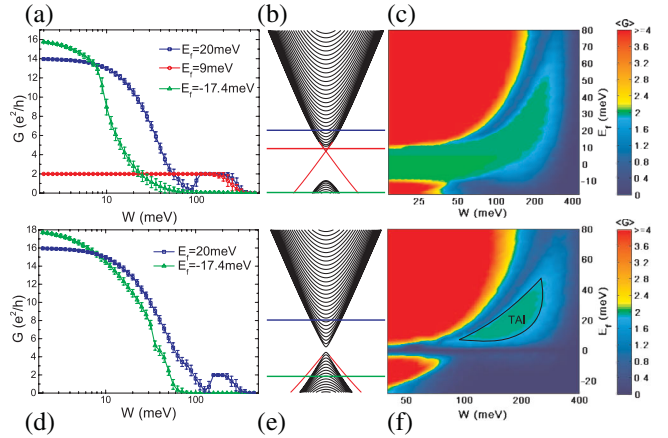


FIG. 2 (color). Conductance of disordered strips of HgTe/CdTe quantum wells. The upper panels (a) to (c) show results for an quantum well inverted with  $M = -10$  meV, and the lower panels (d) to (f) for a normal quantum well with  $M = 1$  meV. (a) The conductance  $G$  as a function of disorder strength  $W$  at three values of Fermi energy. The error bars show standard deviation of the conductance for 1000 samples. (b) Band structure calculated with the tight-binding model. Its vertical scale (energy) is same as in (c) and the horizontal lines correspond to the values of Fermi energy considered in (a). (c) Phase diagram showing the conductance  $G$  as a function of both disorder strength  $W$  and Fermi energy  $E_f$ . The panels (d),(e), and (f) are same as (a),(b), and (c), but for  $M > 0$ . The TAI phase regime is labeled. In all figures, the strip width  $L_y$  is set to  $500 \text{ nm}$ ; the length  $L_x$  is  $5000 \text{ nm}$  in (a) and (d), and  $2000 \text{ nm}$  in (c) and (f).

disordered [green lines in Fig. 2(a) and 2(d)]. The conductance in this case decays to zero at disorder strength around 100 meV, which is about 5 times the conventional hopping energy between nearest neighboring sites  $t = -D/a^2 \approx 20.5$  meV, and much larger than the clean-limit bulk band gap  $E_g = 2|M| = 20$  meV. Here  $a = 5$  nm is the lattice spacing of the tight-binding model. The topological insulator [red line in Fig. 2(a)] is robust, and requires a strong disorder before it eventually yields to a localized state. This is expected as a result of the absence of backscattering in a topological insulator when time-reversal symmetry is preserved [10].

The most surprising aspect revealed by our calculations is the appearance of anomalous conductance plateaus at large disorder for situations when the clean-limit system is a metal without preexisting edge states. See, for example, the blue lines in Fig. 2(a) ( $M < 0$ ) and Fig. 2(d) ( $M > 0$ ). The anomalous plateau is formed after the usual metal-insulator transition in such a system. The conductance fluctuations [the error bar in Fig. 2(a) and 2(d)] are vanishingly small on the plateaus; at the same time the Fano factor drops to nearly zero indicating the onset of dissipationless transport in this system [24], even though the disorder strength in this scenario can be as large as several hundred meV. This state is termed topological Anderson insulator. The quantized conductance cannot be attributed to the relative robustness of edge states against disorder, because it occurs for cases in which no edge states exist in the clean limit. The irrelevance of the clean-limit edge states to this physics is further evidenced from the fact that no anomalous disorder-induced plateaus are seen for the clean-limit metal for which bulk and edge states coexist; those exhibit a transition into an ordinary Anderson insulator.

The nature of TAI is further clarified by the phase diagrams shown in Fig. 2(c) for  $M < 0$  and in Fig. 2(f) for  $M > 0$ . For  $M < 0$ , the quantized conductance region (green area) of the TAI phase in the upper band is connected continuously with the quantized conductance area of the topological insulator phase of the clean limit. One cannot distinguish between these two phases by the conductance value. When  $M > 0$ , however, the anomalous conductance plateau occurs in the highlighted green island labeled TAI, surrounded by an ordinary Anderson insulator. No plateau is seen for energies in the gap, where a trivial insulator is expected. The topology of the TAI phase as well as the absence of preexisting edge states in the clean limit demonstrate that the TAI owes its existence fundamentally to disorder.

The dissipationless character suggests existence of ballistic edge states in the TAI phase. To gain insight into this issue, we investigate how the conductance scales with the width of the strip. Figure 3 shows the calculated conductances of a strip as a function of its width  $L_y$ . In the region before the TAI phase is reached, the scaled conductance  $GL_x/L_y$ , or conductivity, is width independent, as shown

in the inset of Fig. 3, which implies bulk transport. Within the TAI phase, absence of such scaling indicates a total suppression of the bulk conduction, thus confirming presence of conducting edge states in an otherwise localized system.

We further examine the picture of edge-state transport in the TAI phase in a four-terminal cross-bar setup by calculating the spin-resolved transmission coefficients  $T_{pq}^s$  ( $s = \uparrow, \downarrow$ ) between each ordered pair of leads  $p$  and  $q$  ( $= 1, 2, 3, 4$ ). Time-reversal symmetry guarantees that  $T_{pq}^\uparrow = T_{qp}^\downarrow$ , so it suffices to discuss only one spin component  $s = \uparrow$ . Three independent coefficients,  $T_{21}^\uparrow$ ,  $T_{31}^\uparrow$ , and  $T_{41}^\uparrow$ , are shown in Fig. 4 as a function of the disorder strength inside the cross region. The shadowed area marks the TAI phase, where  $\langle T_{41}^\uparrow \rangle = 1$ ,  $\langle T_{21}^\uparrow \rangle = \langle T_{31}^\uparrow \rangle = 0$ , and all transmission coefficients exhibit vanishingly small fluctuations. From symmetry, it follows that  $\langle T_{41}^\uparrow \rangle = \langle T_{24}^\uparrow \rangle = \langle T_{32}^\uparrow \rangle = \langle T_{13}^\uparrow \rangle \rightarrow 1$ , and all other coefficients are vanishing small. These facts are easily understood from the presence of a chiral edge state for the spin up in the TAI phase. Two consequences of this chiral edge state transport are a vanishing diagonal conductance  $G_{xx}^\uparrow = (T_{21}^\uparrow - T_{12}^\uparrow)e^2/h = 0$  and a quantized Hall conductance  $G_{xy}^\uparrow = (T_{41}^\uparrow - T_{42}^\uparrow)e^2/h = e^2/h$ , analogous to Haldane's model for the integer quantum Hall effect with parity anomaly [25]. The quantized Hall conductance  $G_{xy}^\uparrow$  reveals that the topologically invariant Chern number of this state is equal to one [11,26,27]. The absence of Hall current in a time-reversal invariant system implies  $G_{xy}^\uparrow = -G_{xy}^\downarrow = -e^2/h$ . Thus, the chiral edge state in the spin down sector moves in the opposite direction as the edge state in the spin up sector. As a result, the total longitudinal conductance and Hall conductance both vanish as in an ordinary insulator, but the

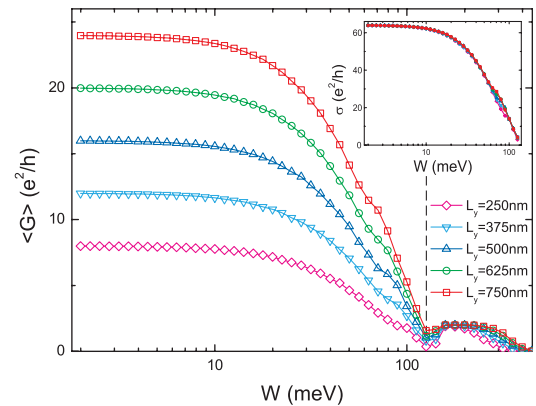


FIG. 3 (color). Width-dependence of the conductance in disordered strips of HgTe/CdTe quantum wells with several values of strip width  $L_y$  and a length  $L_x = 2000$  nm. In the inset, the conductance traces prior to the TAI phase (left-hand-side of the dashed line) are scaled with the width of the strips as  $\sigma = GL_x/L_y$ . The formation of the edge states is indicated by the presence of conductance quantization  $2e^2/h$ . In this figure,  $M = 2$  meV, and the Fermi energy  $E_f = 20$  meV.

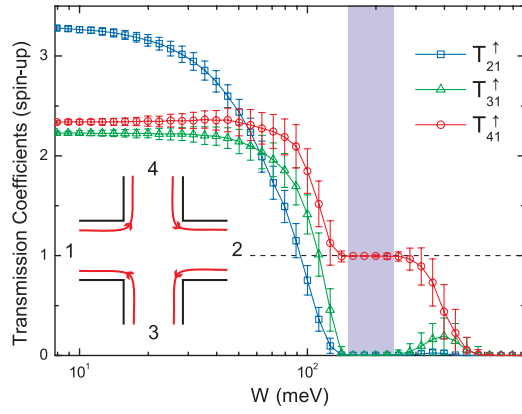


FIG. 4 (color). Three independent spin-resolved transmission coefficients,  $T_{21}^\uparrow$ ,  $T_{31}^\uparrow$ , and  $T_{41}^\uparrow$ , are plotted as functions of the disorder strength  $W$ . Standard deviations of the transmission coefficients for 1000 samples are shown as the error bars. In the shadowed range of disorder strength, all bulk states are localized and only chiral edge states exist, which is schematically shown in the inset (for spin-up component only). The width of leads is 500 nm and  $M = 1$  meV and  $E_f = 20$  meV.

dimensionless spin Hall conductance  $G_{xy}^s = (G_{xy}^\uparrow - G_{xy}^\downarrow)/(e^2/h) = 2$ , resulting in quantum spin Hall effect [8].

Our work thus predicts quantized conductance in the presence of strong disorder even for parameters for which the system is an ordinary metal in the clean limit. The difference between this phase and the previously studied topological insulators is twofold. First, the Fermi energy lies in a region of mobility gap in the bulk, as opposed to a real gap; the mobility gap can be much larger than the clean-limit band gap. Second, the presence of ballistic edge states in the TAI phase does not rely on any band inversion, and hence is not a consequence of band structure. Although the physical origin of these edge states is not clear to us, it is evidently related to the presence of strong disorder in the system. To address this issue further, it is instructive to examine the location of the TAI in the phase diagram by comparing the localization length and the geometrical size of the strongly disordered system. Our one-parameter scaling analysis [28] has found that near the metal-insulator transition, the localization length  $\lambda(W, L_y)$  scales as  $\ln(\lambda/L_y) = \eta(1 - W/W_c)(L_y/a)^{1/\nu} + \ln\Lambda_c$ , where  $W_c \approx 350$  meV is the critical disorder strength in the thermodynamic limit,  $\nu \approx 2.65$  is the localization length exponent,  $\Lambda_c$  is the critical value of the renormalized localization length  $\lambda/L_y$ , and  $\eta$  is a dimensionless constant factor. Evidently no interesting phase exists for  $W > W_c$ , where the conductance is totally suppressed due to exponentially decaying localization length. On the other hand, for  $W < W_c$  the conductance is in principle determined by the ratio of the strip length to  $\lambda$ . For instance, in the situations shown in Fig. 3, the localization length with the disorder strength marked by the dashed line is estimated to be  $\lambda \approx 2.1 \times 10^3$  nm for  $L_y = 250$  nm and  $\lambda \approx 1.5 \times 10^4$  nm for  $L_y = 750$  nm. Considering the strip length  $L_x = 2000$  nm,

it is thus easy to understand the apparently reduced dip with increasing  $L_y$ , prior to the establishment of the TAI phase. This also leads to two interesting cases of the phase diagram: one with the TAI phase surrounded by the normal Anderson insulator phase [Fig. 2(f)] when the strip is long enough, and the other with the TAI phase is connected to the normal metal phase when the strip is wide enough. In either case, the TAI phase is distinguished by the onset of ballistic transport carried only by helical edge states. We believe that HgTe/CdTe quantum wells, which have been used to investigate topological insulators in the clean limit, are a promising candidate also for an experimental determination of the phase diagram of the topological insulator as a function of disorder and doping, because they enable a control of various parameters through variations in the quantum well thickness and gate voltage [29,30].

The authors would like to thank F. C. Zhang and Yshai Avishai for helpful discussions. This work was supported by the Research Grant Council of Hong Kong under Grant No. HKU 7037/08P and HKU 10/CRF/08.

\*Present address: Department of Theoretical Physics, University of Geneva, CH-1211 Geneva 4, Switzerland.

- [1] E. Abrahams *et al.*, Phys. Rev. Lett. **42**, 673 (1979).
- [2] S. Hikami *et al.*, Prog. Theor. Phys. **63**, 707 (1980).
- [3] T. Ando, Phys. Rev. B **40**, 5325 (1989).
- [4] S. V. Kravchenko *et al.*, Phys. Rev. B **50**, 8039 (1994).
- [5] K. v. Klitzing *et al.*, Phys. Rev. Lett. **45**, 494 (1980).
- [6] D. C. Tsui *et al.*, Phys. Rev. Lett. **48**, 1559 (1982).
- [7] S. Das Sarma and A. Pinczuk, *Perspectives in Quantum Hall Effects* (Wiley, New York, 1997).
- [8] C. L. Kane and E. J. Mele, Phys. Rev. Lett. **95**, 226801 (2005).
- [9] B. A. Bernevig *et al.*, Science **314**, 1757 (2006).
- [10] C. L. Kane and E. J. Mele, Phys. Rev. Lett. **95**, 146802 (2005).
- [11] D. J. Thouless *et al.*, Phys. Rev. Lett. **49**, 405 (1982).
- [12] C. Xu and J. E. Moore, Phys. Rev. B **73**, 045322 (2006).
- [13] C. Wu *et al.*, Phys. Rev. Lett. **96**, 106401 (2006).
- [14] M. Onoda *et al.*, Phys. Rev. Lett. **98**, 076802 (2007).
- [15] D. N. Sheng *et al.*, Phys. Rev. Lett. **97**, 036808 (2006).
- [16] M. König *et al.*, Science **318**, 766 (2007).
- [17] L. Fu *et al.*, Phys. Rev. Lett. **98**, 106803 (2007).
- [18] S. Murakami, New J. Phys. **9**, 356 (2007).
- [19] D. Hsieh *et al.*, Nature (London) **452**, 970 (2008).
- [20] M. König *et al.*, J. Phys. Soc. Jpn. **77**, 031007 (2008).
- [21] B. Zhou *et al.*, Phys. Rev. Lett. **101**, 246807 (2008).
- [22] R. Landauer, Philos. Mag. **21**, 863 (1970).
- [23] M. Büttiker, Phys. Rev. B **38**, 9375 (1988).
- [24] M. Büttiker, Phys. Rev. Lett. **65**, 2901 (1990).
- [25] F. D. M. Haldane, Phys. Rev. Lett. **61**, 2015 (1988).
- [26] Q. Niu *et al.*, Phys. Rev. B **31**, 3372 (1985).
- [27] S. S. Lee and S. Ryu, Phys. Rev. Lett. **100**, 186807 (2008).
- [28] A. MacKinnon and B. Kramer, Phys. Rev. Lett. **47**, 1546 (1981); Z. Phys. B **53**, 1 (1983).
- [29] C. R. Becker *et al.*, Phys. Rev. B **62**, 10353 (2000).
- [30] X. C. Zhang *et al.*, Phys. Rev. B **63**, 245305 (2001).